Alkylated chitosans of low molecular weight as non-viral transfection vectors for gene therapy

DATASET *in* RUSSIAN JOURNAL OF GENERAL CHEMISTRY · DECEMBER 2012

Impact Factor: 0.48

9 AUTHORS, INCLUDING:

Alexander Slita
Research Institute of Influenza
20 PUBLICATIONS **85** CITATIONS
SEE PROFILE

Vladimir Zarubaev
Influenza Research Institute
80 PUBLICATIONS **353** CITATIONS
SEE PROFILE

Yves Mély
University of Strasbourg
320 PUBLICATIONS **7,200** CITATIONS
SEE PROFILE

Guy Duportail
University of Strasbourg
66 PUBLICATIONS **1,603** CITATIONS
SEE PROFILE

THE JOURNAL OF GENE MEDICINE
J Gene Med 2008; **10**: 527–539.
Published online 11 February 2008 in Wiley InterScience (www.interscience.wiley.com) **DOI:** 10.1002/jgm.1167

RESEARCH ARTICLE

Hydrophobically modified low molecular weight chitosans as efficient and nontoxic gene delivery vectors

Xin Zhang,[1†] Sebnem Ercelen,[1,2†] Guy Duportail,[1] Emmanuel Schaub,[1] Vladimir Tikhonov,[3] Alexander Slita,[4] Vladimir Zarubaev,[4] Valery Babak,[3] Yves Mély[1]*

[1]*Département de Pharmacologie and Physicochimie, Equipe Photophysique des Interactions Biomoléculaires, Institut Gilbert Laustriat, Faculté de Pharmacie, Université Louis Pasteur, Illkirch, France,* [2]*TUBITAK MRC Genetic Engineering and Biotechnology Institute, Gebze, Kocaeli, Turkey,* [3]*A. Nesmeyanov Institute of Elemento-Organic Compounds (INEOS), Russian Academy of Sciences, Moscow, Russia,* [4]*Influenza Research Institute, Russian Academy of Medical Sciences, Saint-Petersbourg, Russia*

*Correspondence to: Yves Mély, Département de Pharmacologie and Physicochimie, Equipe Photophysique des Interactions Biomoléculaires, Institut Gilbert Laustriat, UMR 7175, Faculté de Pharmacie, Université Louis Pasteur, BP 60024, 67401 Illkirch Cedex, France. E-mail: yves.mely@pharma.u-strasbg.fr

†Both investigators contributed equally and should be considered as senior authors.

Received: 21 November 2007
Revised: 14 December 2007
Accepted: 17 December 2007

Abstract

Background Chitosan derivatives are potential candidates for gene delivery because they are biocompatible and low toxic. However, their use has been limited by their moderate transfection efficiency and the rather large sizes of DNA complexes with high molecular weight chitosans. To circumvent these limitations, we used low molecular weight (approximately 5 kDa) chitosans grafted at 3 and 18 mol% with *N*-/2(3)-(dodec-2-enyl)succinoyl groups (HM-LMW-ch) that exhibit surfactant-like properties.

Methods The physico-chemical properties of complexes of DNA with the two HM-LMW-ch derivatives and the nonmodified LMW-ch were compared by electrophoresis, dynamic light scattering, fluorescence spectroscopy and fluorescence correlation spectroscopy. Moreover, their transfection efficiencies and cytotoxicity were evaluated and their intracellular trafficking was monitored by confocal microscopy. Finally, their ability to deliver genes in mice kidneys after systemic administration was investigated.

Results Complexes with HM(3%)-LMW-ch, but not with HM(18%)-LMW-ch and LMW-ch, efficiently delivered genes in mice kidneys. HM(3%)-LMW-ch formed small positively charged particles that were resistant to DNases and nucleases and marginally interact with serum components. Moreover, these particles were efficiently internalized in cells and low toxic. By contrast, HM(18%)-LMW-ch formed large and weakly charged aggregates with DNA that were highly susceptible to DNases and nucleases.

Conclusions HM(3%)-LMW-ch appears to be a promising nonviral vector with low cytotoxicity and efficient transfection properties. Copyright © 2008 John Wiley & Sons, Ltd.

Keywords chitosan derivatives; confocal microscopy; fluorescence; gene delivery; nonviral gene therapy; transfection

Introduction

The success of gene therapy is mainly limited by the development of vectors able to deliver DNA, used as a therapeutic agent, to targeted cells [1]. Among nonviral vectors, chitosans are good candidates because they are biocompatible and biodegradable, as well as demonstrating low immunogenicity and toxicity [2–5]. Chitosans are naturally occurring polysaccharides (consisting of D-glucosamine and *N*-acetyl β-D-glucosamine linked by $\beta(1 \rightarrow 4)$ glycosidic bonds) that are obtained by alkaline

deacetylation of chitin extracted from crustaceans, insects and fungi [3]. Being cationic polymers, chitosans bind negatively charged DNA and protect it from nuclease degradation [5–9]. Moreover, their complexes with DNA have been successfully applied for *in vitro* transfection assays [9–16] and gene delivery *in vivo* [12,14,17].

However, due to their pK_a value of approximately 6.5 [18] and the hydrophobicity of their glucosamine backbone, the aqueous solubility of chitosans is low at neutral pH, especially in the case of chitosans of high molecular weight. Moreover, high molecular weight chitosans form rather large complexes with DNA [12] that likely prevents their internalization in cells and diffusion through the capillary network. These drawbacks can be partially circumvented by using low molecular weight chitosans (LMW-chs) [2,12,16,19–21], which are water soluble in a large pH range. LMW-chs form small complexes (approximately 100 nm) with DNA but show only moderate transfection efficiency [12]. A significant increase in transfection was obtained by using quaternized LMW-chs that form with DNA complexes of approximately 200–500 nm in diameter [19]. However, their transfection efficiency in differentiated cells is still limited [19,22] and their ability to deliver genes *in vivo* has not been reported. An alternative approach to increase the transfection efficiency of chitosans is to introduce alkyl chains [23] or *N*-acetylcysteine [24]. Optimal transfection was obtained when the number of carbons in the alkyl side chain exceeds eight. However, the solubility of alkylated chitosans was low and their complexes with DNA were micrometric in size, probably due to the rather high molecular weight chitosan and high substitution degree (22%) used in this case.

In this context, to obtain at neutral pH values, soluble chitosan derivatives able to complex DNA into small particles with improved transfection efficiency, we used LMW-ch with moderate alkylation degree (3% and 18%). These hydrophobically modified low molecular weight chitosans (HM-LMW-ch) which have been recently synthesized [25,26], exhibit a mean molecular mass of 5 kDa (approximately 20–25 glucosamine monomers) and a degree of acetylation of 3%. These HM-LMW-ch derivatives are substituted by tetradecenoyl (TDC) chains at 3 and 18% mol (Figure 1), which corresponds to 1 and 5 TDC chains per chitosan molecule, respectively. Due to their relatively low molecular weight and the carboxyl groups associated with the alkyl chains, these samples exhibit a good solubility in water at neutral pH. Moreover, HM-LMW-chs have been shown to exhibit surfactant-like properties by forming micelles with critical micellar concentrations (CMCs) of 0.1–1.1 mM. However, in contrast to surfactants, the HM-LMW-ch exhibit a very low cytotoxicity [26].

In the present study, complexes of DNA with HM-LMW-ch derivatives were characterized and compared with LMW-ch/DNA complexes by electrophoresis, dynamic light scattering, fluorescence spectroscopy and fluorescence correlation spectroscopy (FCS). Moreover, their transfection efficiencies, cytotoxicity and intracellular trafficking, as well as their ability to deliver genes in mice after systemic administration, were investigated. HM(3%)-LMW-ch was found to be a promising nonviral vector showing a good efficiency in delivering genes in mice kidneys.

Materials and methods

Materials

A series of *N*-/2(3)-(dodec-2-enyl)succinoyl/chitosans was prepared by reacting high molecular weight chitosan with 2-(dodecen-1-yl)succinic anhydride (Sigma) [27]. Low molecular weight chitosan and a series of *N*-/2(3)-(dodec-2-enyl)succinoyl/-derivatives were prepared by acidic hydrolysis of high molecular weight chitosans according to a previously described protocol [28]. 1,1′-(4,4,8,8-tetramethyl-4,8-diazaundecamethylene)bis-4-[(3-methylbenz-1,3-oxazol-2-yl)methylidine]-1,4-dihydroquinolinium] tetraiodide (YOYO-1), 5-bromo-4-chloro-3-indolyl-β-D-galactopyranoside (X-Gal) and 2-[3-(diphenylhexatrienyl)propanoyl]-1-hexadecanoyl-sn-glycero-3-phosphocholine (DPHpPC) were from Molecular Probes (Eugene, OR, USA). Polyethylenimine

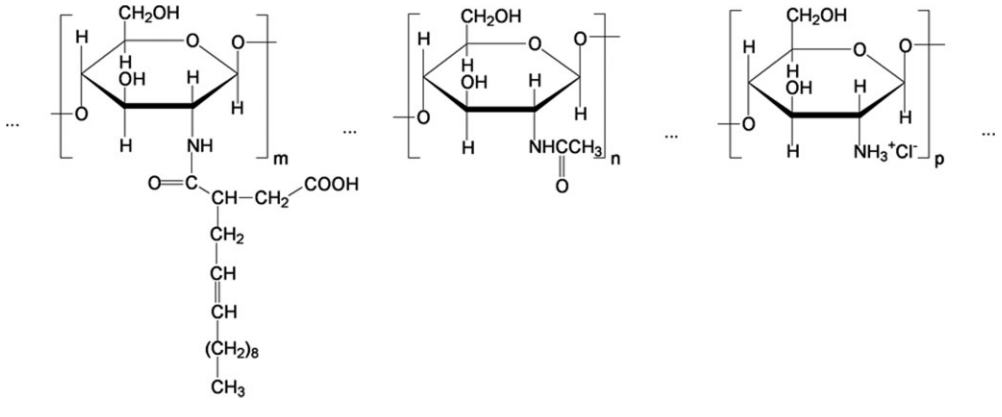

Figure 1. Chemical formula of the HM-LMW-ch derivatives. These derivatives contain unsaturated tetradecenoyl (m), *N*-acetyl (n) and amino-groups (p)

DOI: 10.1002/jgm

(PEI) (25 kDa, branched) was from Sigma Aldrich (St Louis, MO, USA). Calf thymus DNA, dimyristoyl-phosphatidyl-DL-glycerol (DMPG), DNase I, ethidium bromide (EtBr) and Glutaraldehyde were from Sigma Aldrich.

The pCMV-Luc plasmid (5581 bp) encoding luciferase and pUC 19 plasmid (2686 bp) containing a reporter gene of β-galactosidase (LacZ) were grown in *Escherichia coli* and purified by a Qiagen kit (Qiagen, Valencia, CA, USA) [29]. The purity and integrity of the plasmids were assessed by absorption spectroscopy (A_{260}/A_{280} ratio) and electrophoresis on a 1% agarose gel. The DNA concentration was determined by ultraviolet (UV) absorbance at 260 nm, using a Cary 400 (Varian, Mulgrave, Australia) spectrophotometer. The rhodamine-labelled pGeneGrip plasmid was obtained from Gene Therapy Systems (San Diego, CA, USA). Large unilamellar vesicles were prepared by extrusion as described previously [26].

Agarose gel electrophoresis

HM-LMW-ch stock solutions (1 mg/ml) were in 20 mM MES buffer at pH 6.5. The HM-LMW-ch/pDNA complexes were prepared by adding the HM-LMW-ch molecules to the pDNA (0.5 μg) at different N/P ratios (1–10) followed by intense vortexing for 10 s and 30 min incubation at room temperature [15]. The N/P ratio between chitosan and pDNA is expressed as the molar ratio between all protonable amino groups of chitosan and the phosphate groups of pDNA. The HM-LMW-ch/pDNA complexes were then analysed by gel electrophoresis on a 1% agarose gel prepared with 0.5× TAE (Tris-acetate-ethylenediaminetetraacetic acid) buffer containing 1 μg/ml of EtBr [30]. Electrophoresis was carried out with 0.5× TAE buffer at a constant voltage of 100 mV. Plasmid DNA bands were visualized by an UV transilluminator.

For monitoring the protection of complexed pDNA to DNase I and serum, the HM-LMW-ch/pDNA complexes (0.5 μg pDNA) were incubated with 1 U DNase I at 37 °C for 30 min or with 10% foetal bovine serum (FBS) Dubelcco's modified Eagle's medium (DMEM) for 3 h 30 min [8]. The DNase I reaction was stopped by the addition of DNase I stop solution. The integrity of the pDNA was then analysed by gel electrophoresis as described above.

Quasi-elastic light-scattering measurements

The HM-LMW-ch/DNA complexes were prepared with 20 μg of calf thymus DNA and various amounts of HM-LMW-ch in 20 mM MES at various pH and incubated for 30 min at room temperature [15]. The average size of the complexes was determined with a Zetamaster 3000 (Malvern Instruments, Paris, France) with the following specifications: sampling time, 30 s; medium viscosity, 1.054 cP; refractive index (RI) medium, 1.34; RI particle, 1.45; scattering angle, 90°; temperature, 25 °C. The zeta potential of the complexes was measured with the following specifications: sampling time, 30 s; medium viscosity, 1.054 cP; dielectric constant, 80.37; scattering angle, 90°; temperature, 25 °C.

Fluorescence spectroscopy and FCS measurements

Emission spectra were recorded on a Fluorolog (Horiba Jobin-Yvon, Longjumeau, France) spectrofluorimeter. Condensation of DNA by HM-LMW-ch was monitored by using the DNA bis-intercalator YOYO-1 excited at 470 nm [31]. The molar ratio of YOYO-1/DNA base was 1 : 50. DNA/YOYO-1 complexes were obtained by mixing equal volumes of solutions of DNA and YOYO-1 in 20 mM MES buffer at pH 6.5. To ensure a uniform distribution of YOYO-1, the solution was incubated overnight at 4 °C under continuous stirring.

The interaction of HM-LMW-ch/DNA complexes with DMPG vesicles was monitored by using the fluorescence of EtBr which was added at a molar ratio of one EtBr molecule to 50 DNA bases. EtBr was excited at 520 nm. Buffer conditions were as for YOYO-1 experiments.

Steady-state fluorescence anisotropy (r) was measured with a SLM 8000 (SLM Instruments, Urbana, IL, USA.) spectrofluorimeter in the T-format [26]. The DMPG vesicles were labelled with 1% of the fluorescent phospholipid DPHpPC. Excitation was at 360 nm and the emitted light was monitored with 435 nm interference filters. A home-built device ensured the automatic rotation of the excitation polarizer, allowing continuous measurement of the anisotropy. The temperature was regulated with a circulating water bath. The heating rate was fixed at 1 °C/min and the temperature was continuously monitored with a thermocouple inserted into the sample. Pairs of data (r and T °C) were simultaneously recorded and processed with the Biokine software (Biologic, Claix, France). The ratio of the chitosan amine concentration to the concentration of lipid vesicles (expressed in lipids, 0.2 mM) was kept constant at 0.25 in 20 mM MES buffer at pH 6.5.

FCS measurements were performed on a home-built setup as previously described [32,33]. Calibration was performed with a 50 nM tetramethyl-rhodamine (TMR) solution [34]. Assuming a three-dimensional Gaussian distributed excitation intensity, the fluorescence autocorrelation function of free diffusing species can be calculated by:

$$G(\tau) = \frac{1}{N}\left(1+\frac{\tau}{\tau_d}\right)^{-1}\left(1+\frac{1}{S^2}\frac{\tau}{\tau_d}\right)^{-1/2}\left(1+\left(\frac{f_t}{1-f_t}\right)\exp(-\tau/\tau_t)\right) \quad (1)$$

where N is the mean number of molecules in the excitation volume, s is the ratio between the equatorial and axial

DOI: 10.1002/jgm

radii of the focal volume, and τ_d is the correlation time of the particle. τ_t designates the triplet state lifetime and f_t is the mean fraction of fluorophores in the triplet state. The diffusion coefficient, D_{exp}, of the labelled DNA molecules and their complexes was calculated from the comparison with TMR ($D_{TMR} = 2.8 \times 10^{-6}$ cm^2/s) by: $D_{exp} = D_{TMR} \times \tau_{d(TMR)}/\tau_{d(exp)}$, where $\tau_{d(TMR)}$ and $\tau_{d(exp)}$ are the measured correlation times for TMR and the DNA molecules and their complexes, respectively, [34]. FCS data were analysed with Origin (Microcal, Northhampton, MA, USA).

Cell transfection and cytotoxicity

Hela human cervix epitheloid carcinoma cells were grown in DMEM (Gibco BRL, Gaithersburg, MD, USA). DMEM was supplemented with 10% FBS (Cambrex, Charles City, IA, USA), 1% penicillin and streptomycin (Gibco BRL). Cells were maintained at 37 °C in a 5% CO_2 humidified atmosphere. For transfection, *Hela* cells were incubated in serum-free Opti-MEM (Gibco BRL) or DMEM in the presence of 10% FBS with pCMV-Luc plasmid DNA (5 μg/well) complexed with HM-LMW-ch at N/P ratios of 5 and 10. After 3 h 30 min, the transfection medium was replaced with fresh complete medium, and cells were cultured for an additional 24 h. Then, cells were lysed to measure the luciferase gene expression using a commercial kit (Promega, Cergy Pontoise, France) and a luminometer (Mediators PhL, Wien, Austria). Results were expressed as relative light units integrated over 10 s per mg of cell protein lysate (RLU/mg of protein).

Cytotoxicity of HM-LMW-ch/pDNA complexes was evaluated by the 3-(4,5-dimethyl-2-thiazolyl)-2,5-diphenyltetrazolium bromide (MTT; Molecular Probes) assay [35]. *HeLa* cells were seeded at 5×10^4 cells/well in 24-well plates and incubated for 24 h. HM-LMW-ch/pDNA complexes were added to the cells for 24 h. The transfection medium was then replaced with fresh complete medium, and cells were cultured for an additional 24 h. Cells were then washed with phosphate-buffered saline (PBS), and 250 μl of 0.5 mg/ml MTT solution in DMEM was added to each well. Plates were incubated for an additional 1 h at 37 °C. Then, MTT-containing medium was removed and 100 μl of dimethylsulphoxide was added to dissolve the formazan crystals formed by living cells. Absorbance was measured at 535 nm by using a Labsystems iEMS microplate reader (Labsystems, Helsinki, Finland).

Confocal microscopy

Hela cells were cultured as monolayers in 75-cm^2 culture flasks in complete medium. Cells were transferred into a chambered coverglass with 0.8 ml of the same medium and then, after 24 h, with HM-LMW-ch/pDNA complexes that were preformed in 20 mM MES pH 6.5 with 60 μM pDNA (pCMV-Luc) at N/P = 5. The complexes were labelled with YOYO-1 at a ratio of one dye for 300 bases of the pDNA and added to the cells in a 5% CO_2 atmosphere, at 37 °C. After incubation, cells were observed with a Leica TCS SP2 confocal microscope (Leica Microsystems, Wetzlar, Germany).

In vivo experiments

HM-LMW-ch/pDNA (pUC 19; 50 μg) complexes at various N/P ratios were prepared in sterile filtered 20 mM MES buffer at pH 6.5 followed by vortexing for 10 s and incubating 30 min at room temperature. For control experiments, PEI/pDNA complexes were prepared in sterile filtered 150 mM NaCl solution at N/P = 5. Female mice aged between 10 and 12 weeks were anesthetized. Then, 100 μl of the complexes was administered in the tail vein with a needle. Three days after administration, mice were sacrificed, and kidneys were harvested and frozen using liquid nitrogen. Cryostat sections of 11 μm were cut from different lobes of the kidney. The sections were then fixed in PBS containing 0.25% glutaraldehyde at 4 °C for 15 min and washed with PBS. The sections were stained with an X-gal assay at 37 °C for 72 h. The stained sections were washed with PBS and then visualized under a light microscope coupled to a digital camera (Nikon Coolpix 990; Nikon, Tokyo, Japan). Experiments were performed with groups of three mice for each sample.

Results

Physico-chemical characterization of the HM-LMW-ch/DNA complexes

Formation of DNA complexes with LMW-ch and HM-LMW-ch was first monitored by electrophoresis on 1% agarose gel since the neutralization and increase of molecular size that accompanied DNA complexation strongly decreased its electrophoretic mobility [36]. A progressive decrease of the free plasmid band was observed with increasing N/P ratios to the benefit of the retarded band corresponding to the complexes (Figure 2). Complete retardation was observed at N/P ratio of 5, 3 and 2 for LMW-ch, HM(3%)-LMW-ch, and HM(18%)-LMW-ch, respectively. Thus, the recruitment of DNA molecules into the complexes appears to be more efficient when the TDC content increases.

In a second step, the size of the complexes of calf thymus DNA with LMW-ch, HM(3%)-LMW-ch and HM(18%)-LMW-ch at pH 6.5 was measured as a function of N/P ratio by dynamic light scattering (DLS) (Figure 3). The complexes with LMW-ch reached a maximum size (around 800 nm) at N/P = 3, whereas the smallest sizes were obtained at N/P ≥ 5. A similar qualitative dependence of the size of the complexes as a function of N/P was obtained when complexes were formed with HM(3%)-LMW-ch. The only significant difference is the increased size of the complexes at N/P = 3. More striking differences

DOI: 10.1002/jgm

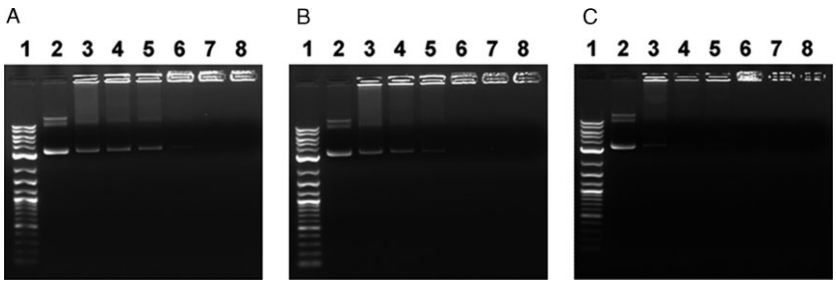

Figure 2. Gel electrophoresis of the pDNA complexes with LMW-ch derivatives. Agarose gels (1%) with (A) LMW-ch, (B) HM(3%)-LMW-ch and (C) HM(18%)-LMW-ch. In all gels, lane 1 corresponds to the molecular weight ladder; lane 2 corresponds to the plasmid DNA control and lanes 3–8 correspond to complexes formed at N/P ratios of 1, 2, 3, 5, 8 and 10, respectively

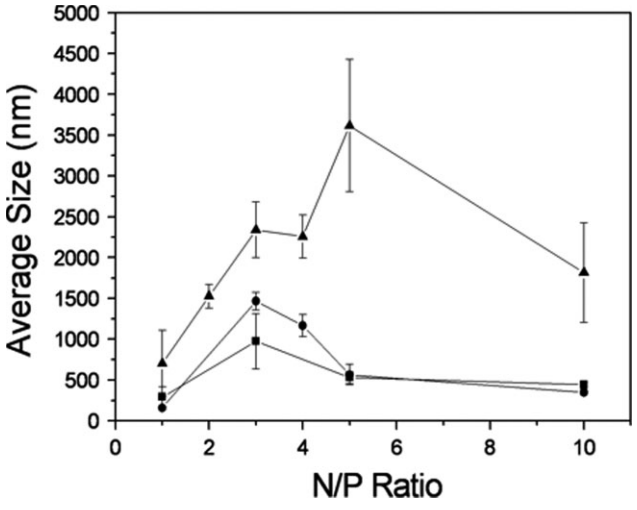

Figure 3. Effect of N/P ratio on the average size of the complexes of DNA with LMW-ch derivatives. LMW-ch/DNA (■), HM(3%)-LMW-ch/DNA (●) and HM(18%)-LMW-ch/DNA (▲) complexes were in 20 mM MES buffer at pH 6.5

appeared with HM(18%)-LMW-ch. First, the N/P ratio at which the complexes with HM(18%)-LMW-ch exhibit their maximum size was shifted to 5. Second, much larger complexes were observed at N/P = 5 (approximately 3500 nm) and N/P = 10 (approximately 1800 nm). As a consequence, the degree of TDC substitution strongly modulates the size of the complexes.

In a next step, the size of the complexes was investigated in a pH range centred around the pK_a value of chitosans [18] (Figure 4A). This study was performed at N/P = 5, a ratio that is commonly used with chitosan derivatives for transfection [37–39]. A very similar behaviour was observed for LMW-ch and HM(3%)-LMW-ch with an increase of the size of the complexes from 100 nm to 1000 nm when pH the increased from 6.2–7.0, indicating that the size was highly dependent on the protonation state of the chitosan derivatives. In the case of HM(18%)-LMW-ch, a sharp increase of the size of the complexes, up to 3800 nm, was observed when pH was increased. In addition, complexes with HM(18%)-LMW-ch were heterogeneous because, for example, two populations at 180 and 450 nm were observed at pH 5.8 (data not shown). Accordingly, these data confirm that the degree of TDC substitution modulates the size of the complexes with DNA.

Next, the zeta potential of the different complexes (N/P = 5) was investigated as a function of pH (Figure 4B). In line with the decrease of the protonation of the chitosan amine groups (and thus the decrease of positive charges) with increasing pH, the zeta potential of all complexes was found to decrease when

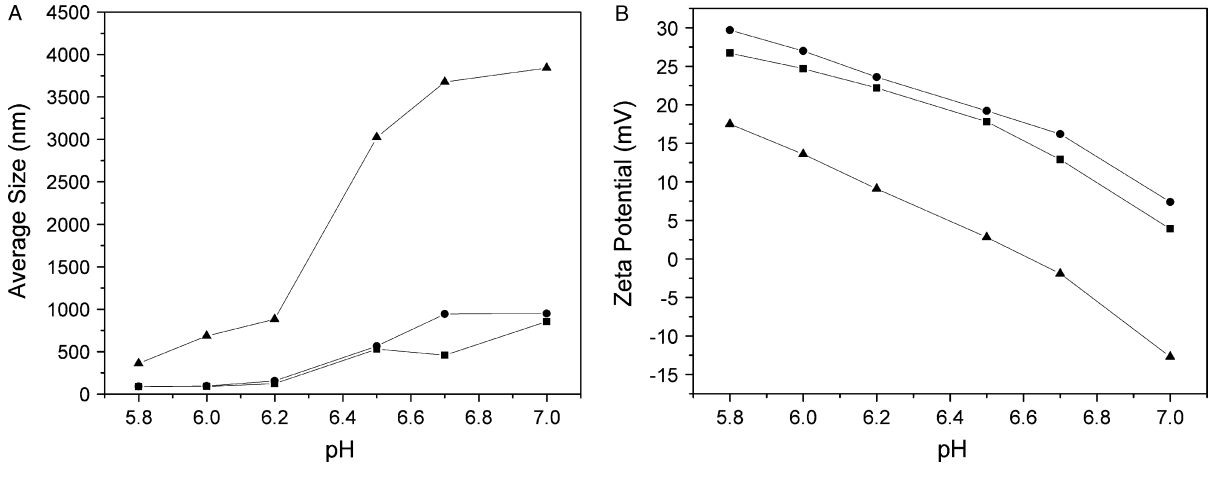

Figure 4. Effect of pH on the average size and zeta potential of the complexes of DNA with LMW-ch derivatives. The average size (A) and zeta potential (B) of the complexes of DNA with LMW-ch (■), HM(3%)-LMW-ch (●) and HM(18%)-LMW-ch (▲) were measured in 20 mM MES buffer

DOI: 10.1002/jgm

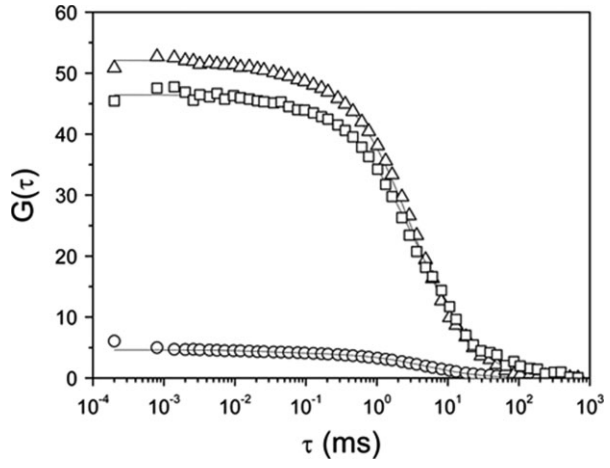

Figure 5. Autocorrelation curves of the complexes of pDNA with LMW-ch derivatives. The concentration of Rh-pDNA was 20 μM. The solid lines correspond to the best fits of the autocorrelation curves of free Rh-pDNA (○), LMW-ch/Rh-pDNA (□) and HM(3%)-LMW-ch/Rh-pDNA (△) complexes. The complexes were formed at N/P = 5

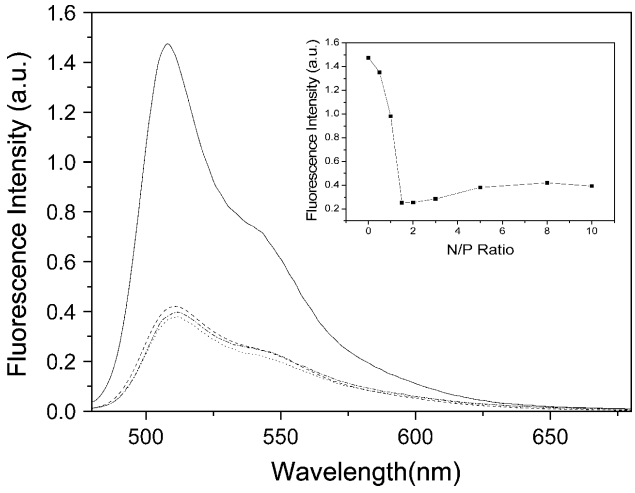

Figure 6. Fluorescence emission spectra of YOYO-1 labelled DNA complexed with the various LMW-ch derivatives. Complexes were formed with LMW-ch (dash line), HM(3%)-LMW-ch (dot line) and HM(18%)-LMW-ch (dash dot line) at N/P = 5. Free YOYO-1 labelled DNA is indicated by the solid line. The concentration of DNA (phosphate) and YOYO-1 were 60 and 1.2 μM, respectively. Inset: Dependence of the YOYO-1/DNA fluorescence intensity at 520 nm on the N/P ratio for HM(3%)-LMW-ch. The buffer was 20 mM MES at pH 6.5. Excitation was at 470 nm

pH was raised. In good agreement with the data shown in Figure 4A, we did not observe any significant difference between LMW-ch/DNA and HM(3%)-LMW-ch/DNA complexes. By contrast, the zeta potentials for the much bigger HM(18%)-LMW-ch/DNA complexes were 10–20 mV lower, indicating a strong relationship between the surface charge and the size of the complexes.

To independently determine the size of the complexes and characterize their composition, we performed FCS experiments using a rhodamine-labelled plasmid (Rh-pDNA) (Figure 5). The autocorrelation curves of the complexes with the chitosan derivatives were adequately fitted by Equation 1, giving the diffusion coefficients shown in Table 1. Since the chitosan/pDNA complexes are mainly globular [20], their hydrodynamic diameter can be deduced from the diffusion coefficients using the Stokes–Einstein equation. For LMW-ch and HM(3%)-LMW-ch, the sizes of the complexes deduced by FCS were in excellent agreement with those determined by DLS (Table 1). In the case of HM(18%)-LMW-ch/Rh-pDNA complexes, reliable autocorrelation curves could not be obtained due to the appearance of big spikes corresponding to large complexes in the fluorescence fluctuations profiles. Formation of the LMW-ch/Rh-pDNA and HM(3%)-LMW-ch/Rh-pDNA complexes was found to decrease the average number of species in the focal volume [$N = 1/G(0)$] with respect to free Rh-pDNA by a factor of 10 and 12, respectively (Figure 5). Moreover, both complexes were approximately eight-fold brighter than free Rh-pDNA. The good consistency between the changes in the number of species and brightness during complexation strongly suggested that: (i) both complexes contain an average of ten pDNA per complex; (ii) the fluorescence intensity of Rh-pDNA is not strongly affected by complexation; and (iii) all pDNA molecules are likely complexed at N/P = 5. In addition, although the complexes contain multiple pDNA copies, they diffuse faster than naked pDNA (Table 1) in line with their expected condensation by the chitosan derivatives.

Table 1. Determination of the number of pDNA in complexes with LMW-ch derivatives and the diameters of these complexes by FCS

Samples	Diffusion constant (m^2/s)	$N_{free}/N_{complex}$[a]	$B_{complex}/B_{free}$[a]	Diameter (nm) by FCS	Diameter (nm) by DLS
Rh-pDNA	2.4×10^{-12}	–	–	–	–
LMW-ch/Rh-pDNA	3.3×10^{-12}	10	7.8	150	100
HM(3%)-LMW-ch/Rh-pDNA	3.9×10^{-12}	12	8.0	120	140

[a] N_{free} and $N_{complex}$ are the number of free pDNA and pDNA in complexes with LMW-ch derivatives, respectively. $N_{free}/N_{complex}$ represents the number of pDNA in complexes with LMW-ch derivatives. B_{free} and $B_{complex}$ are the brightness of free pDNA and the pDNA in complexes, respectively.

To independently assess the condensation of DNA by the chitosan derivatives, the bis-intercalator fluorescent dye YOYO-1 was used [31,40]. Complexation by all three chitosan derivatives at N/P = 5 and pH 6.5 strongly quenched YOYO-1 fluorescence (Figure 6), indicating DNA condensation, in line with the FCS data. Noticeably, a comparison of pDNA with calf thymus DNA revealed that the extent of condensation by the chitosan derivatives was independent of the nature of the DNA (data not shown). Finally, we monitored the quenching of YOYO-1 fluorescence for the complexes with HM(3%)-LMW-ch as a function of N/P ratio at pH 6.5 (Figure 6, inset). A continuous fluorescence quenching was observed up to N/P = 1.5–2, where a minimum was reached. This suggested that, at this ratio, all the DNA molecules were

DOI: 10.1002/jgm

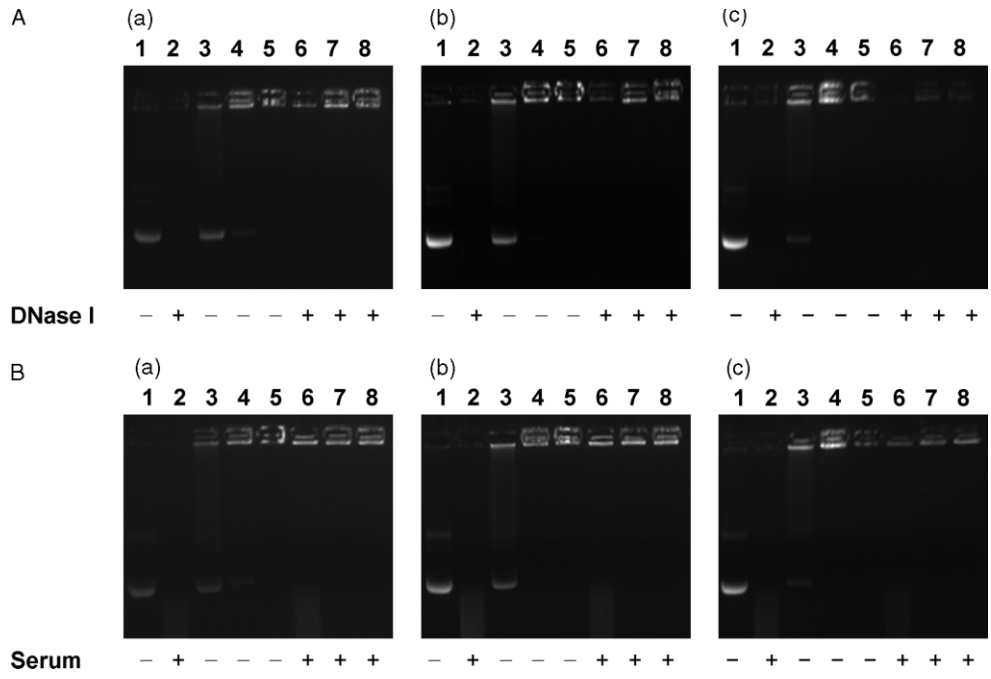

Figure 7. (A) DNase I and (B) serum protection assays. Complexes of pDNA (0.5 μg) with (a) LMW-ch, (b) HM(3%)-LMW-ch and (c) HM(18%)-LMW-ch were formed at various N/P ratios. Complexes were incubated either with (+) or without (−) DNase I (1 U) at 37 °C for 30 min (A) and 10% FBS medium for 3 h 30 min (B). Then, degradation of pDNA was monitored by 1% agarose gel electrophoresis. In all gels, lanes 1 and 2 correspond to pDNA control, lanes 3–8 correspond to the complexes with N/P ratios of 1 (lanes 3 and 6), 5 (lanes 4 and 7) and 10 (lanes 5 and 8), respectively

complexed by HM(3%)-LMW-ch molecules, in agreement with the electrophoresis data shown in Figure 2B. At higher N/P ratios, a small fluorescence recovery was observed.

In the last step, the protection degree of pDNA in the complexes against DNase I and serum was examined (Figures 7A and 7B). Naked pDNA showed a complete degradation when incubated with 1 U DNase I for 30 min at 37 °C or with 10% FBS medium for 3 h 30 min. At N/P = 1, the fraction of pDNA not included in the complexes was rapidly degraded by DNase I and the serum nucleases. By contrast, the pDNA included in the complexes (top bands of the gels) with LMW-ch and HM(3%)-LMW-ch at all N/P ratios were protected against both DNase I and serum. Surprisingly, no protection against DNase I and only partial protection against the serum nucleases was observed in the complexes with HM(18%)-LMW-ch. This suggests that the internal arrangement in the HM(18%)-LMW-ch/pDNA complexes is different from the two other ones, enabling the access of the enzymes to the pDNA molecules.

Interaction of the HM-LMW-ch/DNA complexes with model membranes

Since the HM-LMW-ch molecules have previously been shown to interact with negatively charged vesicles, mimicking the internal leaflet of the plasma membrane [26], we tested whether their complexes with pDNA could also interact with these vesicles. To this end, the interaction of the various complexes at N/P ratios of 1 and 5 with DMPG anionic vesicles was monitored through the thermotropic fluorescence anisotropy profiles of the DPHpPC-labelled vesicles (Figures 8A to 8C). We also investigated the condensation state of DNA within the complexes by using EtBr (Figures 8D to 8F). Upon DNA condensation, EtBr is expelled from DNA, causing a decrease in the fluorescence signal [41]. In the absence of vesicles, a limited decrease of EtBr fluorescence was observed when DNA was complexed with the chitosan derivatives at N/P = 1. In line with the electrophoresis data (Figure 2), this suggests that part of the DNA remained in a free form. In further agreement with the electrophoresis data, the EtBr fluorescence, and thus the amount of free DNA, was the lowest with HM(18%)-LMW-ch. At N/P = 5, the low EtBr fluorescence observed with all complexes confirmed that nearly all DNA molecules were complexed.

The thermotropic anisotropy profiles of DMPG vesicles in the presence of the different chitosan derivatives and their complexes with DNA at pH 6.5 are shown in Figures 8A to 8C. We confirmed that all chitosan derivatives, by themselves, stabilized DMPG vesicles as seen by the increase of both T_m ($\Delta T_m = +3$ °C) and fluorescence anisotropy in the liquid crystalline phase. With the complexes at N/P = 1, no significant change in the thermotropic curves and EtBr fluorescence was observed, suggesting no interactions with the complexes at this ratio. By contrast, both the LMW-ch/DNA and HM(3%)-LMW-ch/DNA complexes at N/P = 5 stabilized the DMPG vesicles to the same extent as the corresponding free chitosan molecules. Meanwhile, only a small increase

DOI: 10.1002/jgm

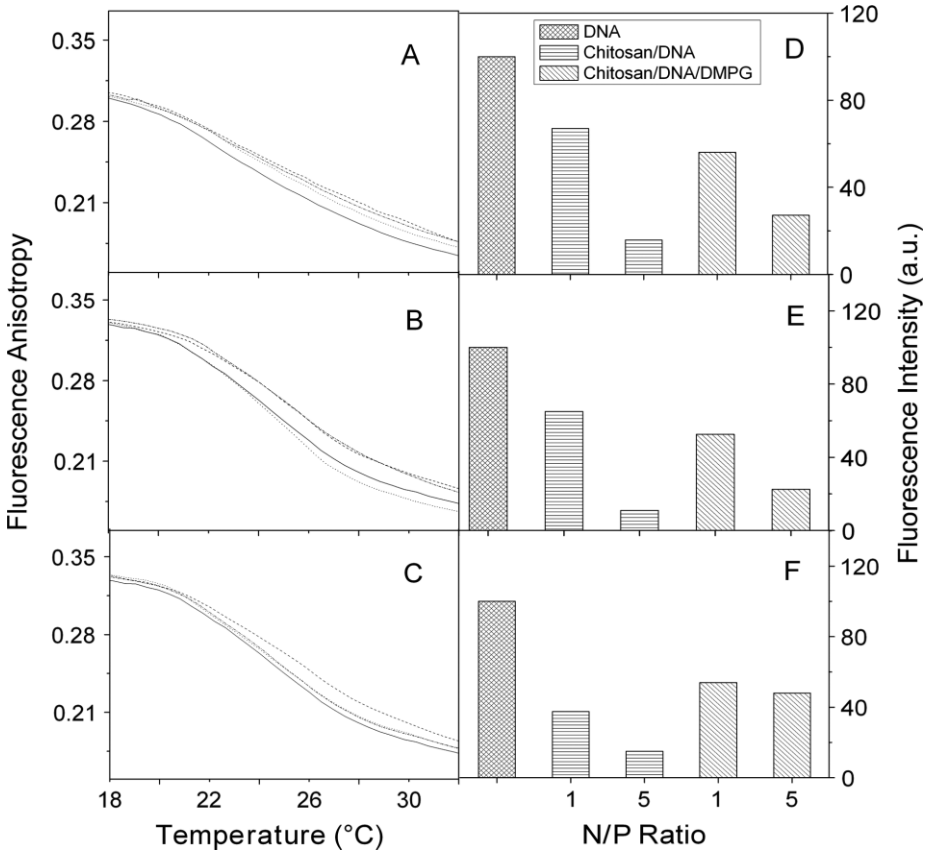

Figure 8. Interaction of LMW-ch/DNA and HM-LMW-ch/DNA complexes with DMPG large unilamellar vesicles. (A–C) Fluorescence anisotropy thermotropic curves. The interaction was monitored with complexes of DNA with (A) LMW-ch, (B) HM(3%)-LMW-ch and (C) HM(18%)-LMW-ch. The thermotropic curves were recorded with DPHpPC- labelled DMPG vesicles in the absence (solid line) or in the presence of the free chitosan derivative (dash line) and its DNA complexes at N/P = 1 (dotted line) and 5 (dash–dot line). (D–F) EtBr intercalation monitored by its fluorescence intensity. EtBr-labelled DNA was complexed with (D) LMW-ch, (E) HM(3%)-LMW-ch and (F) HM(18%)-LMW-ch. EtBr was excited at 520 nm. The DNA/EtBr molar ratio was 50 : 1. In all experiments, the molar ratio of LMW-ch derivatives to phospholipid was 0.25 and the final concentration of DMPG vesicles was 200 μM in 20 mM MES buffer at pH 6.5

of EtBr fluorescence was observed in these conditions, suggesting that only a small amount of DNA was decondensed, and thus only a limited amount of the chitosan derivatives was released. Accordingly, the changes in the thermotropic curves may be attributed to the interaction of the nondissociated complexes with the DMPG vesicles. A different behaviour was observed with the HM(18%)-LMW-ch/DNA complexes because only a limited change in the thermotropic curves was perceived. Meanwhile, the EtBr fluorescence increase indicated a significant decondensation of DNA and, thus, a release of HM(18%)-LMW-ch molecules. Consequently, HM(18%)-LMW-ch/DNA complexes may transiently interact with DMPG vesicles and release HM(18%)-LMW-ch molecules that may be responsible for the small changes in the thermotropic curves.

Noticeably, neither of the complexes modified the thermotropic curves of neutral DMPC vesicles (data not shown). In addition, no change in EtBr fluorescence was observed in these conditions. Thus, the various complexes appear to marginally interact with neutral vesicles.

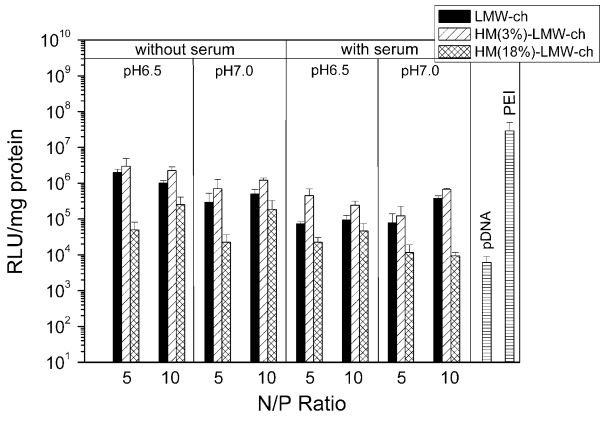

Figure 9. Transfection efficiency of the complexes of DNA with LMW-ch derivatives. *HeLa* cells were incubated in serum-free Opti-MEM or DMEM in the presence of 10% FBS with plasmid DNA complexed with LMW-ch derivatives at pH 6.5 and 7.0, and N/P = 5 and 10. After 3 h 30 min, the transfection medium was replaced with fresh complete culture medium, and cells were cultured for an additional 24 h. Then cells were lysed for luciferase activity quantification. Gene expression determined from the luciferase assay was expressed as RLU/mg of protein

DOI: 10.1002/jgm

In vitro transfection efficiency and intracellular delivery of HM-LMW-ch/pDNA complexes

Transfection experiments with the three chitosan derivatives complexed with pDNA at different N/P ratios (5 and 10) and pH (6.5 and 7) were performed on *HeLa* cells either in the absence or in the presence of serum (Figure 9). In the absence of serum, the LMW-ch/pDNA and HM(3%)-LMW-ch/pDNA complexes at pH 6.5 showed comparable transfection efficiencies (approximately 2×10^6 RLU/mg protein) at both N/P ratios. These efficiencies were approximately 400-fold higher than the control (naked DNA) and only one order of magnitude below the efficiency obtained with branched PEI/pDNA complexes. HM(18%)-LMW-ch/pDNA complexes were clearly less efficient because their transfection efficiency exceeded the control by only eight- and 40-fold for N/P ratios of 5 and 10, respectively. A small decrease in transfection efficiency was observed with all complexes when the pH was raised to 7.

Addition of serum only moderately lowered the transfection efficiency of both LMW-ch/pDNA and HM(3%)-LMW-ch/pDNA complexes. However, a clear difference in the two complexes appeared at pH 6.5 because the transfection efficiency of the HM(3%)-LMW-ch/pDNA complexes exceeded that of the LMW-ch/pDNA complexes by 20- and five-fold for N/P ratios of 5 and 10, respectively. By contrast, the difference between the two complexes almost disappeared at pH 7.0.

Cell viability was also tested in the presence of the various complexes. In all cases, a high level of living cells ($\geq$85%) was found (data not shown), in line with the low cytotoxicity of chitosan [26].

To further understand the transfection efficiency results, the intracellular trafficking of the complexes of YOYO-1-labelled pDNA with the various chitosan derivatives was monitored by confocal microscopy

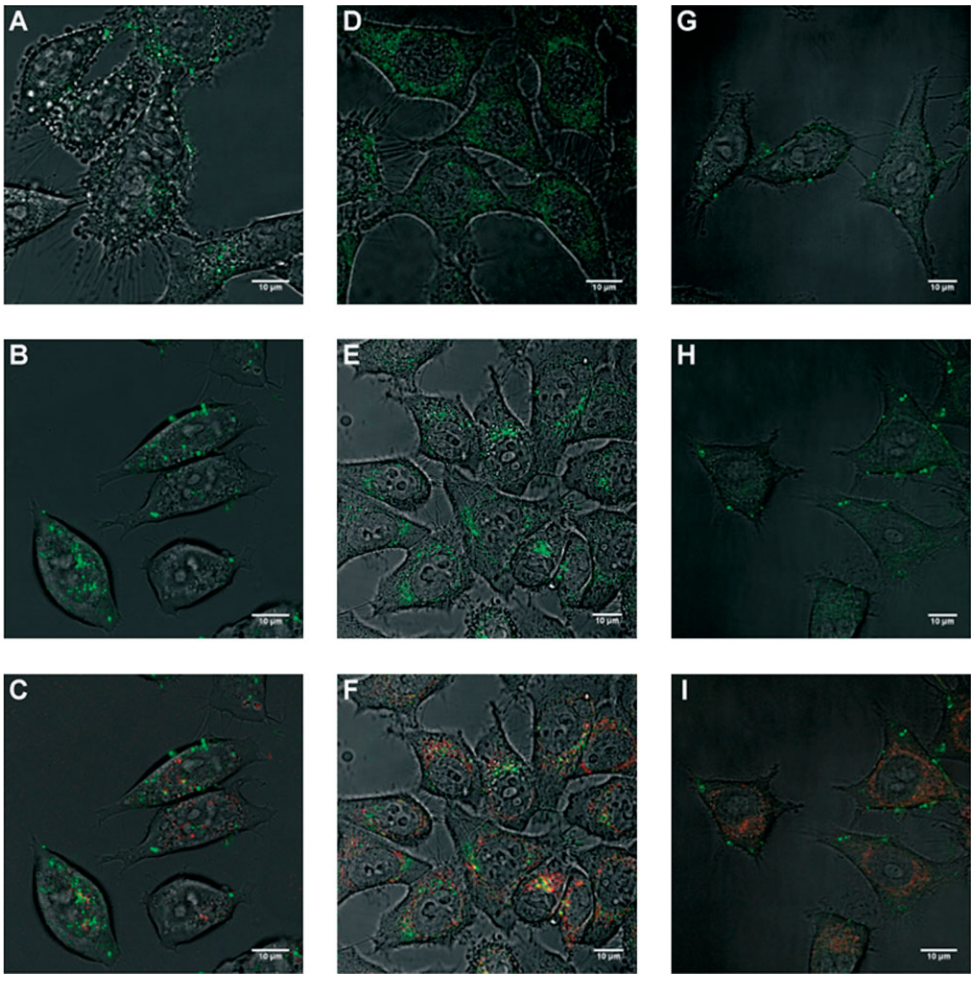

Figure 10. Internalization of the complexes of DNA with the LMW-ch derivatives in *HeLa* cells. The complexes were formed with (A–C) YOYO-1-labelled pDNA and LMW-ch, (D–F) HM(3%)-LMW-ch or (G–I) HM(18%)-LMW-ch, respectively. The concentration of pDNA was 60 μM and the N/P ratio was 5. The images correspond to the overlay of light transmission and fluorescence confocal images and were taken at 30 min (A, D, G) and 3 h 30 min (B, C, E, F, H, I) post transfection. In (C), (F) and (I), FM4-64 was incubated first for 20 min with *HeLa* cells. The cells were then washed and incubated with serum-free Opti-MEM. After 2 h, YOYO-1-labelled complexes were added. Yellow spots correspond to areas where the complexes and FM4-64 are co-localized. Red and green spots correspond to areas containing only FM4-64 and YOYO-1 labelled complexes, respectively. Images are representative of more than 90% of the observed cells. Scale bars = 10 μm

(Figure 10). The complexes were prepared at N/P = 5 at pH 6.5. The intracellular pathway of the complexes was followed after 30 min (Figures 10A, 10D and 10G) and 3 h 30 min (Figures 10B, 10E and 10H) post transfection of *HeLa* cells.

After 30 min, the LMW-ch/pDNA complexes were perceived as rather large aggregates both in the cytoplasm and close to the cell surface (Figure 10A). Large aggregates were also observed with the HM(18%)-LMW-ch/pDNA complexes, but only close to the cell surface (Figure 10G). By contrast, the HM(3%)-LMW-ch/pDNA complexes were distributed as numerous small spots within the cell cytoplasm (Figure 10D), suggesting that they are efficiently internalized.

At 3 h 30 min after addition, the LMW-ch/pDNA complexes were still perceived as large aggregates, but more of them were observed in the cytoplasm (Figure 10B) compared to 30 min post transfection (Figure 10A). Moreover, the HM(18%)-LMW-ch/pDNA aggregates remained mainly localized close to the cell surface (Figure 10H). Again, a distinct feature was observed with the HM(3%)-LMW-ch/pDNA complexes that accumulated in perinuclear areas (Figure 10E). The patterns observed with the latter and their dependence with time suggest internalization of the HM(3%)-LMW-ch/pDNA complexes through endocytosis. To confirm this, we incubated *HeLa* cells with YOYO-labelled particles and FM4-64, a marker of membrane endocytosis [42]. These two dyes can be followed simultaneously because the FM4-64 red fluorescence is easily distinguished from the YOYO-1 green fluorescence. In this respect, co-localization of FM4-64 and the chitosan/pDNA complexes will yield yellow spots. In line with our expectations, we observed punctuated yellow dots which grew in number and size with time (data not shown) and accumulated in perinuclear areas at 3 h 30 min post-transfection (Figure 10F), confirming an internalization of the HM(3%)-LMW-ch/pDNA complexes through endocytosis. By contrast, only a limited number and almost no yellow spots were perceived with LMW-ch/pDNA and HM(18%)-LMW-ch/pDNA complexes, respectively (Figures 10C and 10I).

In vivo transfection studies

To further characterize the HM-LMW-ch derivatives, we investigated their ability to deliver genes *in vivo* after systemic administration. Since the kidney receives approximately 25% of the blood coming from the heart each time it beats, this organ can trap foreign pDNA molecules (through its filtration and concentration function) more easily than other organs (e.g. spleen and heart) [43]. Therefore, we compared the efficiency of the three chitosan derivatives to mediate β-galactosidase gene expression in mice kidneys 3 days after injection into the tail vein. In the presence of ferricyanide and ferrocyanide at neutral pH, the β-galactosidase enzyme converts the substrate X-gal to an intense blue product. Thus, if the pUC 19 plasmid encoding the β-galactosidase gene is taken up by the cells of any tissue, its expression will result in an intense blue colour [43].

In a first step, LMW-ch/pDNA complexes with N/P ratios of 1, 5 and 10 were administered to screen the optimal N/P ratio for *in vivo* transfection. Only for N/P = 5, a faint but reproducible expression was observed 3 days after injection into the tail vein of all the treated mice (Figure 11A). As a consequence, this N/P ratio was selected for investigating the *in vivo* transfection efficiency of the complexes with the HM-LMW-ch derivatives. Interestingly, a very strong expression of the gene was observed after administration of the complexes with HM(3%)-LMW-ch (Figure 11B). This expression was even far more intense than that obtained using branched PEI (Figure 11D), showing that this modified chitosan efficiently delivers the plasmid into the kidney. By sharp contrast, no gene expression was observed when complexes with HM(18%)-LMW-ch were administrated (Figure 11C). As for naked pDNA (Figure 11E), no coloration appeared. Consequently, *in vivo* gene delivery is critically dependent on the degree of TDC substitution.

Discussion

In the present study, we characterized the physico-chemical and transfection properties of complexes of DNA with several LMW-ch derivatives. In addition to the nonmodified LMW-ch derivative, two hydrophobically modified derivatives substituted with 3 and 18% mol TDC groups, respectively, were used. These HM(3%)-LMW-ch and HM(18%)-LMW-ch molecules are highly soluble and, on average, contain one and five TDC chains per chitosan molecule, respectively.

The three chitosan derivatives exhibited substantial differences in their transfection efficiency *in vivo* and in cellular assays. HM(3%)-LMW-ch appears by far the most interesting derivative because it shows a high transfection efficiency *in vivo* via systemic administration. Its efficiency was found to be even better than that of branched PEI, which is a rather efficient vector for *in vivo* applications [44]. By contrast, LMW-ch showed only a limited ability to deliver the plasmid in the mice kidney whereas HM(18%)-LMW-ch was completely inactive. Similar differences in the transfection efficiencies of the various complexes were also observed in cellular assays at pH 6.5, in the presence of serum (Figure 9), suggesting that at least a part of the *in vivo* observations is related to the interaction of the complexes with the cells and their intracellular fate. In line with this hypothesis, we found that only the HM(3%)-LMW-ch/pDNA complexes are readily and efficiently internalized mainly through endocytosis (Figure 10). This may in turn be related to the small size of these complexes in the cell medium because, at 30 min post transfection, the HM(3%)-LMW-ch/pDNA complexes appear as small dots scattered in the cytoplasm (Figure 10A). In the same conditions, both

DOI: 10.1002/jgm

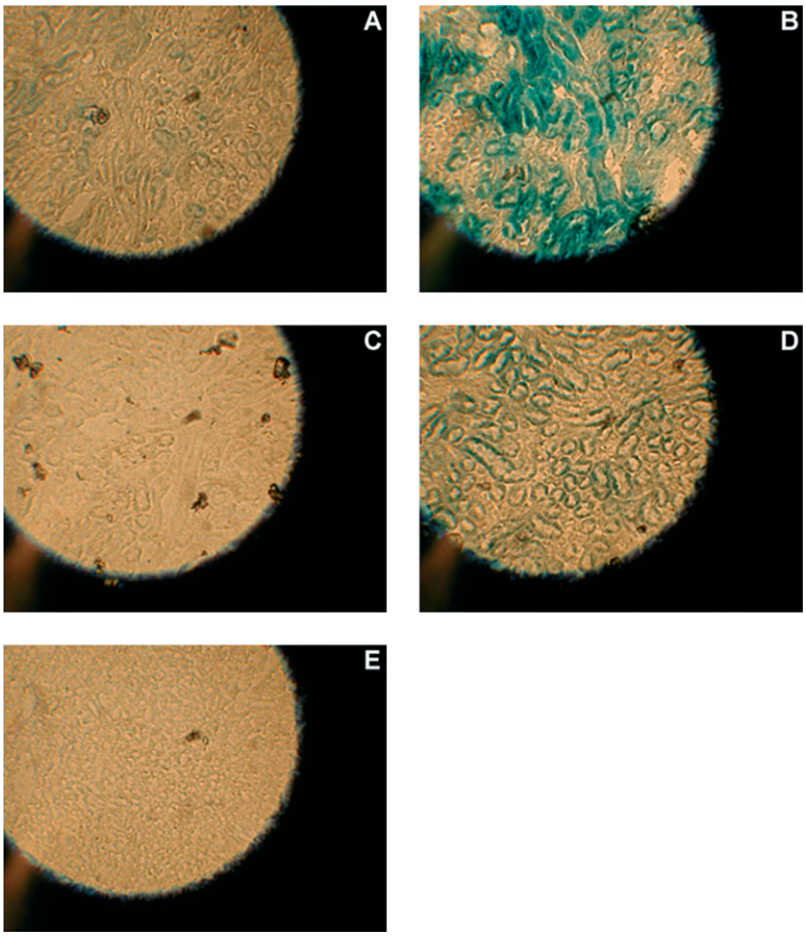

Figure 11. Gene expression in mice kidneys after systemic injection of the complexes of pDNA with the LMW-ch derivatives. Complexes of pUC 19 DNA with (A) LMW-ch, (B) HM(3%)-LMW-ch, (C) HM(18%)-LMW-ch and (D) branched PEI at N/P = 5 were injected into the tail vein of the mice. The kidneys were harvested 3 days after administration. (E) Naked plasmid DNA was injected as a control. Magnification, ×200

LMW-ch/pDNA and HM(18%)-LMW-ch/pDNA complexes form rather large patches that are far less efficiently internalized. This is especially true for the HM(18%)-LMW-ch/pDNA complexes, which remain close to the plasma membrane, even at 3 h 30 min post transfection, explaining their poor transfection efficiency. Similarly, the limited transfection efficiency of the LMW-ch/pDNA complexes may be related to their rather inefficient internalization through endocytosis, as shown by their limited accumulation in perinuclear compartments and limited co-localization with an endocytosis marker (Figures 10D and 10G). By contrast, the differences in the transfection efficiencies of the various complexes could not be related to differences in cytoxicity because all of them were poorly cytotoxic, in line with previous data showing that none of these derivatives was cytotoxic in the free form [26].

Differences in the transfection properties and intracellular trafficking of the various complexes are likely related to differences in their physico-chemical and biochemical properties. The relatively low transfection efficiency of the HM(18%)-LMW-ch/DNA complexes is probably due to their large sizes (Figures 3 to 5). These sizes may be rationalized by the decrease of the charge density of chitosans, consecutive to the covalent modification of on the average five amine groups by TDC, which decreases the ability of the modified chitosans to neutralize the negative charges of DNA. Moreover, each TDC chain contains a carboxylic group that is probably negatively charged at neutral pH, and thus further decreases the cationic character of the HM(18%)-LMW-ch molecules. The decrease in the charge density of HM(18%)-LMW-ch in respect with the two other derivatives is illustrated by the shift in the N/P ratio from 3 to 5 to obtain the maximum size of the complexes at pH 6.5 (Figure 3). Since maximum sizes are obtained when the complexes are neutral, and thus do no more repulse each other due to electrostatic forces, a larger number of the less charged HM(18%)-LMW-ch molecules is needed to neutralize the DNA charges, explaining this shift in the N/P ratio. In addition, as described for other alkylated chitosans [23], inter-molecular interactions through hydrophobic interactions between the TDC chains may further increase the size of the HM(18%)-LMW-ch/DNA complexes. The large size of these complexes probably limits their transportation in the blood stream and extravasation through small vascular fenestrations as well as their diffusion through tissue and cellular uptake [15,45], largely explaining their poor transfection

DOI: 10.1002/jgm

both *in vivo* (Figure 11) and *in vitro* (Figure 9). In addition, the HM(18%)-LMW-ch/pDNA complexes differ from the complexes with the two other chitosan derivatives by their high susceptibility to DNase I and serum nucleases. This high susceptibility is likely related to the surfactant-like properties of HM(18%)-LMW-ch that enable it to form pseudo-micellar structures when bound to DNA, similarly to other surfactants [41,46,47]. In these structures, large portions of the DNA molecules are on the surface of the complexes and, thus, highly accessible to the enzymes. This hypothesis is also consistent with the low surface charge of the complexes. The high susceptibility of the DNA molecules to both the blood nucleases and the intracellular DNase I additionally explains the low transfection efficiency of HM(18%)-LMW-ch/pDNA complexes *in vivo* and in cellular assays in the presence of serum.

The differences in transfection efficiencies of the HM(3%)-LMW-ch/pDNA and LMW-ch/pDNA complexes are more difficult to rationalize on the basis of their properties. Indeed, the two complexes exhibited similar sizes, surface charge, composition in number of DNA plasmids, and insensitivity to DNase I and nucleases. This suggests that the coupling on the average of one TDC group per chitosan molecule is insufficient to significantly modify its charge density and to promote the formation of pseudo-micellar domains. Nevertheless, the TDC chains may favour hydrophobic interactions between the complexes, explaining the increase of size of the complexes at N/P ratios where the complexes are nearly neutral (Figure 3). The TDC chains at the surface of the HM(3%)-LMW-ch/DNA complexes do not appear to affect their interaction with the membranes (Figure 8) because both HM(3%)-LMW-ch/DNA and LMW-ch/DNA complexes do not interact with neutral model membranes and interact similarly with negatively charged model membranes. By analogy to lipoplexes [48], the interaction with the negatively charged phospholipids at the inner face of the endosomes may be a favourable feature for endosome destabilization and release of the complexes in the cytoplasm. In fact, the TDC chains appear critical for limiting the growth of the complexes in biological media, such as serum and cell culture medium, as could be seen from the poor sensitivity of the transfection efficiency of the HM(3%)-LMW-ch/pDNA complexes on serum (Figure 9) and from the comparison of the confocal images for the LMW-ch/pDNA (Figures 10A, 10D and 10G) and HM(3%)-LMW-ch/pDNA (Figures 10B, 10E and 10H) complexes. The TDC chains probably limit the interaction with components that promote the aggregation of the complexes or destabilize them. These components remain to be identified. The observed effects of TDC chains are not unprecedented because alkylation with C_{18} chains has recently been reported to strongly increase the transfection efficiency of dendrimers in the presence of serum [49].

In conclusion, HM(3%)-LMW-ch appears as a promising vector for gene therapy. This chitosan derivative is not cytotoxic and forms small positively charged complexes with DNA that are insensitive to nucleases and DNase I. These positively charged complexes are stable, and not dissociated by interaction with membranes. In addition, they are unaffected by serum and are efficiently internalized through endocytosis, giving rather high transfection efficiencies in cells. The complexes likely remain small when injected through the systemic route and efficiently cross the physiological barriers, explaining their high transfection efficiency in mice kidneys.

Acknowledgements

We thank Marcel Boeglin from the Institut de Génétique et de Biologie Moléculaire et Cellulaire for his help in confocal microscopy. This work was supported by the Agence Française contre les Myopathies (AFM) and the Eco-Net program between France, Russia and Ukraine from the French Ministère des Affaires Etrangères. S.E. is a fellow from the AFM. V.B. is an invited Professor of the Université Louis Pasteur. X.Z. is a fellow from the European Doctoral College.

References

1. Borchard G. Chitosans for gene delivery. *Adv Drug Deliv Rev* 2001; **52**: 145–150.
2. Richardson SCW, Kolbe HVJ, Duncan R. Potential of low molecular mass chitosan as a DNA delivery system: biocompatibility, body distribution and ability to complex and protect DNA. *Int J Pharm* 1999; **178**: 231–243.
3. Illum L. Chitosan and its use as a pharmaceutical excipient. *Pharm Res* 1998; **15**: 1326–1331.
4. Muzzarelli RAA, Belcher R, Freiser H (eds). *Natural Chelating Polymers: Alginic Acid, Chitin, and Chitosan*. Pergamon Press: Oxford, NY, 1973; 144–176.
5. Mansouri S, Lavigne P, Corsi K, Benderdour M, Beaumont E, Fernandes JC. Chitosan-DNA nanoparticles as non-viral vectors in gene therapy: strategies to improve transfection efficacy. *Eur J Pharm Biopharm* 2004; **57**: 1–8.
6. Venkatesh S, Smith TJ. Chitosan–membrane interactions and their probable role in chitosan-mediated transfection. *Biotechnol Appl Biochem* 1998; **27**: 265–267.
7. Cui Z, Mumper RJ. Chitosan-based nanoparticles for topical genetic immunization. *J Control Release* 2001; **75**: 409–419.
8. Huang M, Fong CW, Khor E, Lim L-Y. Transfection efficiency of chitosan vectors: effect of polymer molecular weight and degree of deacetylation. *J Control Release* 2005; **106**: 391–406.
9. Mao H-Q, Roy K, Troung-Le VL, *et al*. Chitosan-DNA nanoparticles as gene carriers: synthesis, characterization and transfection efficiency. *J Control Release* 2001; **70**: 399–421.
10. Corsi K, Chellat F, Yahia LH, Fernandes JC. Mesenchymal stem cells, MG63 and HEK293 transfection using chitosan-DNA nanoparticles. *Biomaterials* 2003; **24**: 1255–1264.
11. Sato T, Ishii T, Okahata Y. In vitro gene delivery mediated by chitosan. effect of pH, serum, and molecular mass of chitosan on the transfection efficiency. *Biomaterials* 2001; **22**: 2075–2080.
12. MacLaughlin FC, Mumper RJ, Wang J, *et al*. Chitosan and depolymerized chitosan oligomers as condensing carriers for in vivo plasmid delivery. *J Control Release* 1998; **56**: 259–272.
13. Ishii T, Okahata Y, Sato T. Mechanism of cell transfection with plasmid/chitosan complexes. *Biochim Biophys Acta* 2001; **1514**: 51–64.
14. Köping-Höggård M, Tubulekas I, Guan H, *et al*. Chitosan as a nonviral gene delivery system. Structure–property relationships and characteristics compared with polyethylenimine in vitro and after lung administration in vivo. *Gene Ther* 2001; **8**: 1108–1121.
15. Erbacher P, Zou S, Bettinger T, Steffan A-M, Remy J-S. Chitosan-based vector/DNA complexes for gene delivery: biophysical characteristics and transfection ability. *Pharm Res* 1998; **15**: 1332–1339.

16. Lee M, Nah J-W, Kwon Y, Koh JJ, Ko KS, Kim SW. Water-soluble and low molecular weight chitosan-based plasmid DNA delivery. *Pharm Res* 2001; **18**: 427–431.
17. Köping-Höggård M, Vårum KM, Issa M, *et al*. Improved chitosan-mediated gene delivery based on easily dissociated chitosan polyplexes of highly defined chitosan oligomers. *Gene Ther* 2004; **11**: 1441–1452.
18. Schipper NG, Vårum KM, Artursson P. Chitosans as absorption enhancers for poorly absorbable drugs. 1: Influence of molecular weight and degree of acetylation on drug transport across human intestinal epithelial (Caco-2) cells. *Pharm Res* 1996; **13**: 1686–1692.
19. Thanou M, Florea BI, Geldof M, Junginger HE, Borchard G. Quaternized chitosan oligomers as novel gene delivery vectors in epithelial cell lines. *Biomaterials* 2002; **23**: 153–159.
20. Köping-Höggård M, Mel'nikova YS, Vårum KM, Lindman B, Artursson P. Relationship between the physical shape and the efficiency of oligomeric chitosan as a gene delivery system in vitro and in vivo. *J Gene Med* 2003; **5**: 130–141.
21. Issa MM, Köping-Höggård M, Tømmeraas K, *et al*. Targeted gene delivery with trisaccharide-substituted chitosan oligomers in vitro and after lung administration in vivo. *J Control Release* 2006; **115**: 103–112.
22. Kean T, Roth S, Thanou M. Trimethylated chitosans as non-viral gene delivery vectors: cytotoxicity and transfection efficiency. *J Control Release* 2005; **103**: 643–653.
23. Liu WG, Zhang X, Sun SJ, Sun GJ, Yao KD. N-alkylated chitosan as a potential nonviral vector for gene transfection. *Bioconjug Chem* 2003; **14**: 782–789.
24. Loretz B, Thaler M, Bernkop-Schnurch A. Role of sulfhydryl groups in transfection? A case study with chitosan-NAC nanoparticles. *Bioconjug Chem* 2007; **18**: 1028–1035.
25. Tikhonov VE, Stepnova EA, Babak VG, *et al*. Bactericidal and antifungal activities of a low molecular weight chitosan and its N-/2(3)-(dodec-2-enyl)succinoyl/-derivatives. *Carbohyd Polym* 2006; **64**: 66–72.
26. Ercelen S, Zhang X, Duportail G, *et al*. Physicochemical properties of low molecular weight alkylated chitosans: a new class of potential nonviral vectors for gene delivery. *Colloids Surf B: Biointerfaces* 2006.; **51**: 140–148.
27. Hirano S, Ohe Y, Ono H. Selective N-acylation of chitosan. *Carbohyd Res* 1976; **47**: 315–320.
28. Domard A, Carter N. Preparation, separation and characterization of the D-glucosamine oligomer series. In *Chitin and Chitosan: Sources, Chemistry, Biochemistry, Physical Properties and Applications*, Skjak-Braek G, Anthonsen T, Sandford P (eds). Elsevier Applied Science: London, 1989; 383–387.
29. Zanta M-A, Boussif O, Adib A, Behr J-P. In vitro gene delivery to hepatocytes with galactosylated polyethylenimine. *Bioconjug Chem* 1997; **8**: 839–844.
30. Kiang T, Wen J, Lim HW, Leong KW. The effect of the degree of chitosan deacetylation on the efficiency of gene transfection. *Biomaterials* 2004; **25**: 5293–5301.
31. Krishnamoorthy G, Duportail G, Mély Y. Structure and dynamics of condensed DNA probed by 1,1′-(4,4,8,8-tetramethyl-4,8-diazaundecamethylene)bis[4-[[3-methylbenz-1,3-oxazol-2-yl] methylidine]-1,4-dihydroquinolinium] tetraiodide fluorescence. *Biochemistry* 2002; **41**: 15277–15287.
32. Clamme J-P, Azoulay J, Mély Y. Monitoring of the formation and dissociation of polyethylenimine/DNA complexes by two photon fluorescence correlation spectroscopy. *Biophys J* 2003; **84**: 1960–1968.
33. Clamme J-P, Krishnamoorthy G, Mély Y. Intracellular dynamics of the gene delivery vehicle polyethylenimine during transfection: investigation by two-photon fluorescence correlation spectroscopy. *Biochim Biophys Acta* 2003; **1617**: 52–61.
34. Egelé C, Schaub E, Piémont É, Rocquigny H, Mély Y. Investigation by fluorescence correlation spectroscopy of the chaperoning interactions of HIV-1 nucleocapsid protein with the viral DNA initiation sequences. *CR Biol* 2005; **328**: 1041–1051.
35. Mosmann T. Rapid colorimetric assay for cellular growth and survival: application to proliferation and cytotoxicity assays. *J Immunol Methods* 1983; **65**: 55–63.
36. Zelikin AN, Putnam D, Shastri P, Langer R, Izumrudov VA. Aliphatic ionenes as gene delivery agents: elucidation of structure-function relationship through modification of charge density and polymer length. *Bioconjug Chem* 2002; **13**: 548–553.
37. Hashimoto M, Morimoto M, Saimoto H, Shigemasa Y, Sato T. Lactosylated chitosan for DNA delivery into hepatocytes: the effect of lactosylation on the physicochemical properties and intracellular trafficking of pDNA/chitosan complexes. *Bioconjug Chem* 2006; **17**: 309–316.
38. Kim TH, Ihm JE, Choi YJ, Nah JW, Cho CS. Efficient gene delivery by urocanic acid-modified chitosan. *J Control Release* 2003; **93**: 389–402.
39. Yu H, Chen X, Lu T, *et al*. Poly (L-lysine)-graft-chitosan copolymers: synthesis, characterization, and gene transfection effect. *Biomacromolecules* 2007; **8**: 1425–1435.
40. Krishnamoorthy G, Roques B, Darlix J-L, Mély Y. DNA condensation by the nucleocapsid protein of HIV-1: a mechanism ensuring DNA protection. *Nucleic Acids Res* 2003; **31**: 5425–5432.
41. Clamme J-P, Bernacchi S, Vuilleumier C, Duportail G, Mély Y. Gene transfer by cationic surfactants is essentially limited by the trapping of the surfactant/DNA complexes onto the cell membrane: a fluorescence investigation. *Biochim Biophys Acta* 2000; **1467**: 347–361.
42. Rémy-Kristensen A, Clamme J-P, Vuilleumier C, Kuhry J-G, Mély Y. Role of endocytosis in the transfection of L929 fibroblasts by polyethylenimine/DNA complexes. *Biochim Biophys Acta* 2001; **1514**: 21–32.
43. Kuemmerle NB, Lin P-S, Krieg RJ Jr, Lin K-C, Ward KP, Chan JCM. Gene expression after intrarenal injection of plasmid DNA in the rat. *Pediatr Nephrol* 2000; **14**: 152–157.
44. Lungwitz U, Breunig M, Blunk T, Göpferich A. Polyethylenimine-based non-viral gene delivery systems. *Eur J Pharm Biopharm* 2005; **60**: 247–266.
45. Kircheis R, Wagner E. Polycation/DNA complexes for in vivo gene delivery. *Gene Ther Regul* 2000; **1**: 95–114.
46. Llères D, Dauty E, Behr J-P, Mély Y, Duportail G. DNA condensation by an oxidizable cationic detergent. Interactions with lipid vesicles. *Chem Phys Lipids* 2001; **111**: 59–71.
47. Dauty E, Rémy J-S, Blessing T, Behr J-P. Dimerizable cationic detergents with a low cmc condense plasmid DNA into nanometric particles and transfect cells in culture. *J Am Chem Soc* 2001; **123**: 9227–9234.
48. Xu Y, Szoka FC Jr. Mechanism of DNA release from cationic liposome/DNA complexes used in cell transfection. *Biochemistry* 1996; **35**: 5616–5623.
49. Takahashi T, Kojima C, Harada A, Kono K. Alkyl chain moieties of polyamidoamine dendron-bearing lipids influence their function as a nonviral gene vector. *Bioconjug Chem* 2007; **18**: 1349–1354.

DOI: 10.1002/jgm